

A level set method and a heat transfer model implemented into FLUENT for modeling of microscale two phase flows

Bogdan Alexandru Nichita*

John Richard Thome*

*Ecole Polytechnique Federale de Lausanne, ME G1 464, Station 9, CH-1015, Switzerland

bogdan.nichita@epfl.ch, john.thome@epfl.ch

ABSTRACT

Thermal design and simulation of two-phase cooling of avionics onboard military aircraft requires extensive analysis to better understand the effects of channel orientation, gravitational effects and transients on thermal performance. Such analysis requires a robust numerical code that can model the fundamental phenomena, while also benchmarked versus known solutions and published experimental data. This paper thus describes the successful implementation of a level set method and a heat transfer model into FLUENT for modeling of adiabatic and evaporating two phase flows. The level set method belongs to the so called 'one' fluid methods where a single set of conservation equations are solved for the whole domain and the interface between the two phases is tracked or captured. FLUENT has already a 'one' fluid method for modeling two phase flows, namely volume-of-fluid, which is then coupled here with the level set method. The resulting coupled level set volume-of-fluid method is superior to both standalone methods by retaining the advantages of each method (better accuracy in computing curvature and normal to the interface for the level set method and precise mass conservation for the volume-of-fluid method). The level set function is used to compute the surface tension contribution to the momentum equations, via curvature and its normal to the interface, using the Brackbill method [1], while the volume of fluid function is used to capture the interface itself. A re-initialization equation is implemented and solved at every time step using a fifth order weighted essentially non-oscillatory (WENO) scheme for the spatial derivative, and a first order Euler method for time integration. The coupling effect is introduced by solving at the end of each time step an equation which connects the volume fractions with the level set function. The detail description is presented in [2]. A heat transfer model was presently implemented into this FLUENT code for solving problems involving boiling or condensation. Besides the Navier-Stokes equations, a energy equation was solved in the whole domain, including the gas phase, and the temperature for the cells containing the interface was set to the saturation one. In boiling or condensation a mass transfer across the interface occurs and this has been handled in the model. This was specified using User Defined Functions (UDFs) as a mass source in the continuity equation. As a first step, a vapor bubble growing inside a microchannel during flow boiling of water is simulated in the present study. A parametric study is performed by varying the static contact angle.

1.0 INTRODUCTION

In the last decade or so, micro two-phase flows have become an alternative to the existing cooling solutions in industry, due to its capacity to remove large thermal densities using a relatively small quantity of refrigerant. Consequently, nowadays it is studied intensively, both experimentally and numerically. Two approaches exist for modeling of two-phase flows: 'one' fluid methods and 'two' fluid methods. In 'one' fluid methods, a single set of conservation equations is solved and the interface is tracked or captured. In 'two' fluid methods, a set of conservation equations is solved for each phase and the

A LS method and a HT model implemented into FLUENT for modeling of two phase flows

interaction between phases is given by some correlations.

Interface tracking methods explicitly track the interface with marker particles like in MAC (marker and cell) methods [3], arbitrary Lagrangian-Eulerian (ALE) methods [4-6], or front tracking methods [7-8]. These methods are very accurate and efficient for flexible moving boundaries with small deformations. However, their main drawback is that they are difficult to use in cases where the interface breaks up or coalesces with another interface. Also additional re-meshing is needed when a large deformation of the interface occurs.

In interface capturing methods, an auxiliary function is needed. These methods are very robust and have a wide range of applicability. However, they require higher mesh resolution. Examples include volume-of-fluid (VOF) [9-12] and level set (LS) methods [13-16].

In VOF methods, the interface is given implicitly by a color function, which is defined as the volume fraction of one of the fluids within each cell. From this function, a reconstruction of the interface is made and the interface is then propagated implicitly by updating the color function. VOF methods are conservative and can deal with topological changes of the interface. However, VOF methods cannot accurately compute several important properties, such as curvature and normal to the interface.

In LS methods, the interface is represented by the zero contour of a continuous signed distance function; this is known as the level set function. The movement of the interface is governed by a transport equation for the level set function. To keep the level set function as a signed distance function, a re-initialization process is needed. LS methods automatically deal with topological changes. It is generally easy to obtain a high order of accuracy just by using an ENO (Essentially non-Oscillatory) or WENO (Weighted Essentially non-Oscillatory) scheme. However, LS methods are not conservative, so that a significant, physically incorrect loss or gain of mass occurs for incompressible two phase flow. Several authors have overcome this problem by coupling the LS and VOF methods [17–24]. In such coupled level set volume of fluid (CLSVOF) techniques, the level set function is used to accurately compute the curvature and the normal to the interface while the volume of fluid function is used to capture the interface. Normally, a CLSVOF method is more accurate than both the standalone LS and VOF methods.

In this paper, we implemented a LS method inside FLUENT and coupled it with the existing VOF method to create a CLSVOF method which improved FLUENT capabilities to simulate two-phase flows. A heat transfer with phase change was also implemented inside FLUENT. The rest of the paper is organized as follows: Section 2 describes briefly the mathematical models, Section 3 presents several numerical results and conclusions are given in Section 4.

2. MATHEMATICAL MODELS

2.1 CLSVOF method

Since VOF method is already implemented and well documented inside FLUENT, in this section the focus will be on the LS method. In this work we perform a direct numerical simulation, so we need to solve the continuity equation and Navier-Stokes equations:

$$\frac{\partial \rho}{\partial t} + \nabla \cdot \rho \mathbf{u} = 0 \quad (2.1)$$

$$\frac{\partial(\rho \mathbf{u})}{\partial t} + \nabla \cdot (\rho \mathbf{u} \otimes \mathbf{u}) = -\nabla p + \nabla \cdot (2\mu \mathbf{D}) + \rho \mathbf{g} + \mathbf{F}_{st} \quad (2.2)$$

A LS method and a HT model implemented into FLUENT for modeling of two phase flows

where in Eq. 2.1 and 2.2 ρ is the density, t is the time, μ is the dynamic viscosity, \mathbf{u} is the velocity vector, \mathbf{g} is the gravity vector, \mathbf{D} is the rate of deformation tensor and \mathbf{F}_{st} is the surface tension force.

It is worth mentioning that ρ and μ are discontinuous. To express them we used a smoothed Heaviside function:

$$H_\varepsilon(\phi) = \begin{cases} 0 & \text{if } \phi < -\varepsilon \\ (\phi + \varepsilon)/(2\varepsilon) + \sin(\pi\phi/\varepsilon)/(2\pi) & \text{if } |\phi| \leq \varepsilon \\ 1 & \text{if } \phi > \varepsilon \end{cases} \quad (2.3)$$

$$\begin{aligned} \rho &= \rho_g + (\rho_l - \rho_g)H_\varepsilon \\ \mu &= \mu_g + (\mu_l - \mu_g)H_\varepsilon \end{aligned} \quad (2.4)$$

where ε is half of the interface thickness and the subscripts l and g denote liquid and gas phases, respectively.

The LS function, which is initialized as the signed distance to the interface (positive in the liquid phase and negative in the gas phase), is then advected with the velocity field:

$$\frac{\partial \phi}{\partial t} + \mathbf{u} \cdot \nabla \phi = 0 \quad (2.5)$$

The surface tension term in Eq. 2.2 is approximated using the CSF (Continuum Surface Force) model of Brackbill [1] using the following relation:

$$\mathbf{F}_{st} = \sigma k(\phi) \mathbf{n} \delta_\varepsilon(\phi) \quad (2.6)$$

where σ is the surface tension coefficient, $k(\phi)$ is the mean curvature of the interface, and \mathbf{n} is the normal vector to the interface, as defined by:

$$\mathbf{n} = \frac{\nabla \phi}{|\nabla \phi|}, \quad k(\phi) = \nabla \cdot \frac{\nabla \phi}{|\nabla \phi|}$$

Furthermore, $\delta_\varepsilon(\phi)$ is the smoothed delta function, which is defined as the derivative of $H_\varepsilon(\phi)$ with respect to ϕ .

After advecting Eq. 2.5, the LS function stops to be a signed distance to the interface, so the LS method needs to reinitialize ϕ at every time step:

$$\frac{\partial \phi}{\partial \tau} + \text{sign}(\phi_0)(|\nabla \phi| - 1) = 0, \quad \phi(x, 0) = \phi_0 \quad (2.7)$$

It is evident that we need the level set function to be a signed distance just near the interface, so usually Eq. 2.7 is solved for $\tau = 0 \dots \varepsilon$. To discretize the gradients in Eq. 2.7 one needs to use a higher order scheme like ENO or WENO [26], otherwise oscillations of the interface occur. In this work we used a fifth order WENO scheme to discretize the gradients in Eq. 2.7.

As we mentioned before, the LS method tends to lose mass. To overcome this problem, we coupled LS with VOF. In other words, since both LS and VOF refer to the same interface, the new interface location should coincide using either LS or VOF functions. The following equation is solved:

$$(\phi + \varepsilon)/(2\varepsilon) + \sin(\pi\phi/\varepsilon)/(2\pi) = F_l \quad (2.8)$$

where F_l is the liquid volume fraction.

A LS method and a HT model implemented into FLUENT for modeling of two phase flows

2.2 Heat transfer with phase change

For solving problems involving heat transfer, besides the Navier-Stokes equations Eq. 2.1 and 2.2, the energy equation is also required:

$$\rho c_p \left(\frac{\partial T}{\partial t} + \mathbf{u} \cdot \nabla T \right) = \nabla \cdot k \nabla T \quad (2.9)$$

Most previous work assumed that the vapor phase remains at the saturation temperature and therefore Eq. 2.9 was not solved in the gas phase. However, this is not necessarily true, especially if the bubble is in contact with a heated wall. In this study the energy equation is also solved in the gas phase and the temperature of the vapor-liquid interface is maintained at the saturation value. In cases of phase change, a mass transfer across the interface occurs and this has been handled inside the model. The mass source for the vapor in case of boiling is:

$$S_g = \frac{(k_g F_g + k_l F_l)(\nabla T \cdot \nabla F_l)}{h_{fg}} \quad (2.9)$$

where in Eq. 2.9 k refers to the thermal conductivity of the fluids, F refers to the volume fraction of the fluids and h_{fg} is the latent heat.

The liquid mass source has the following form:

$$S_l = -S_g$$

There is also a source term in the energy equation:

$$S_e = -S_g \cdot h_{fg}$$

3. NUMERICAL RESULTS

In the first part of this section we show the results obtained with our CLSVOF method and in the last part of this section, a series of simulations involving boiling inside microchannels will be presented.

3.1 CLSVOF results

3.1.1 Verification cases

In order to verify that Eq. 2.7 and 2.8 were implemented correctly, we performed a simulation that consisted of a bubble rising in a viscous fluid due to gravity. In the present study, calculations were performed on a 2D computational domain of 0.08x0.1 m. The bubble was placed at (0.04, 0.02) m and had a radius of 0.005 m. The no slip wall boundary condition was used for all boundaries. The physical properties of the fluids used are presented in Table 3.1. Figure 1 depicts the level set function inside the domain after 0.2 s when solving the re-initialization equation after each time step. In Fig. 2 the same level set function inside the domain is plotted after 0.2s. It is clear that in the first case (Fig. 1) the re-initialization equation is solved correctly and the level set function is a signed distance to the interface. With Fig. 2 we proved that the level set function ceased to be a signed distance to the interface when advecting the level set equation (Eq. 2.1). Figure 3 shows the bubble contour with both LS and VOF functions when solving the coupling equation (Eq. 2.8) after 0.2s. In Fig. 4 the same contours are shown without the coupling between LS and VOF. Again it is clear that: (i) LS method lost a significant fraction of the mass and (ii) by coupling LS with VOF one can conserve mass in case of a LS method.

A LS method and a HT model implemented into FLUENT for modeling of two phase flows

Properties	Density kg / m^3	Viscosity Ns / m^2	Surface tension N / m
Liquid	1000	0.1	0.1
gas	10	0.001	

Table 1: Physical properties of the fluids.

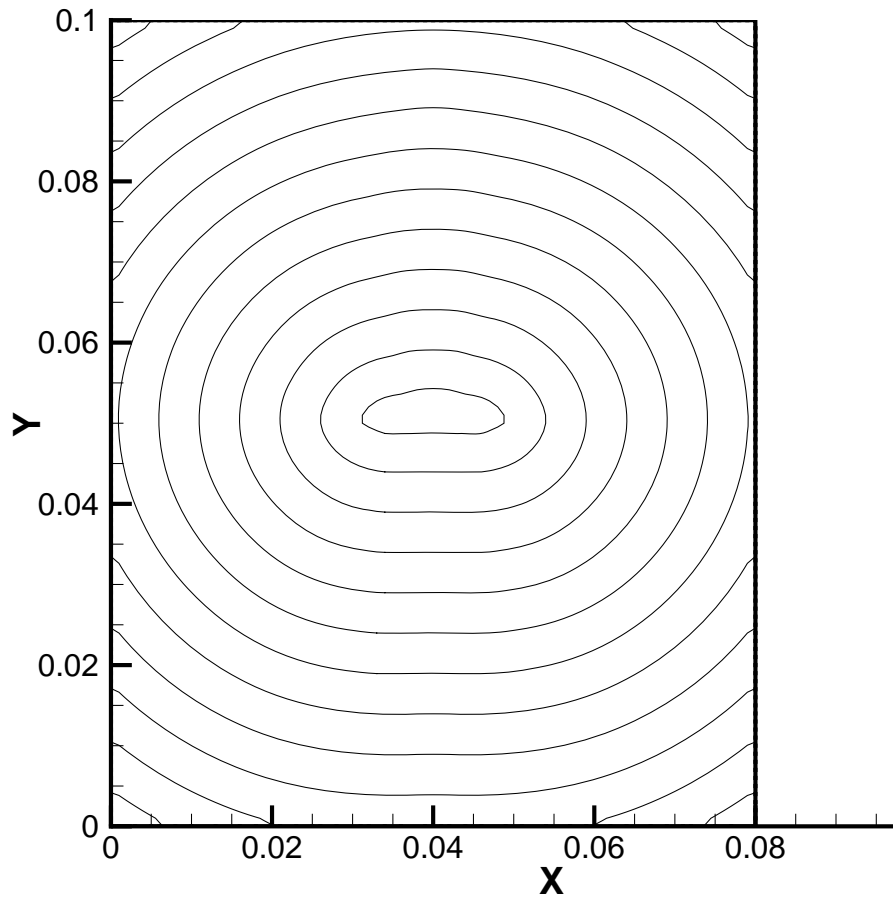


Figure 1: The level set function after solving the re-initialization equation.

A LS method and a HT model implemented into FLUENT for modeling of two phase flows

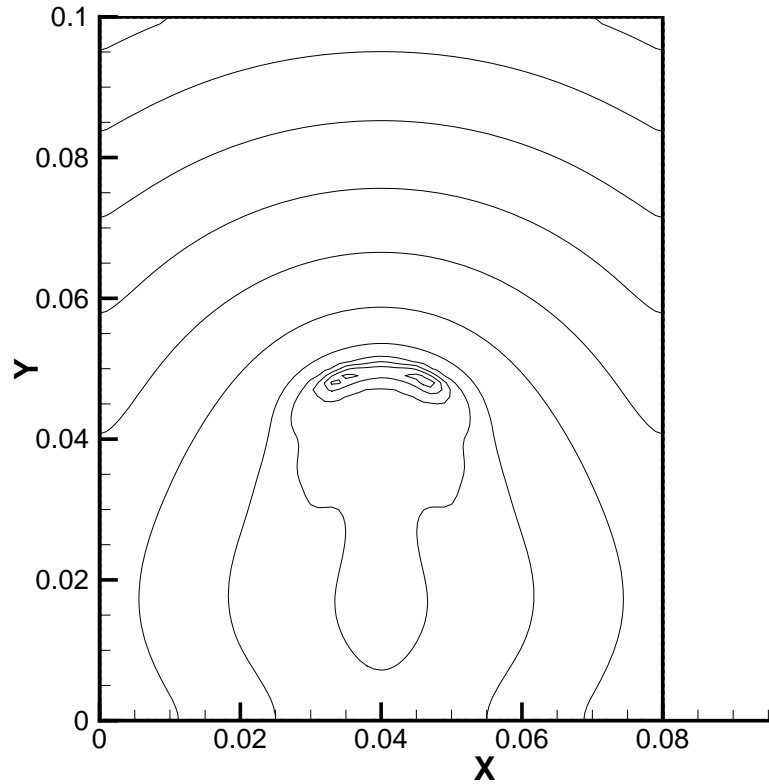


Figure 2: The level set function without solving the re-initialization equation.

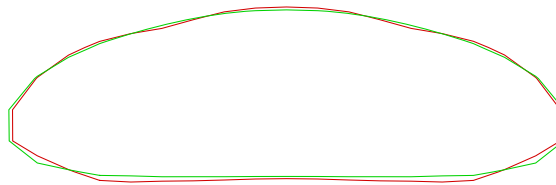


Figure 3: Level set contour (red) and volume-of-fluid contour (green) after solving the coupling equation between LS and VOF.

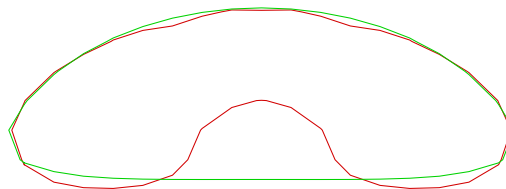


Figure 4: Level set contour (red) and volume-of-fluid contour (green) without coupling between LS and VOF (with large loss of mass).

A LS method and a HT model implemented into FLUENT for modeling of two phase flows

3.1.2 Film thickness simulations

The estimation of the liquid film thickness inside small channels is a key factor for the prediction of flow boiling heat transfer. In this section, the results obtained with elongated air bubbles flowing inside a 1mm diameter tube filled with ethanol are presented, and compared with several correlations found in the literature. In one of these, Han and Shikazono [25] performed a series of film thickness measurements inside circular channels with tube diameters ranged from 0.3 to 1.3 mm with air, ethanol, water and FC-40 as working fluids. In order to have a similar set-up as in the experiments, three air bubbles were used in the present simulation. A 2D domain of 30x1mm was used with a mesh of 3000x100. The implemented CLSVOF method was used. At the inlet, a velocity boundary condition was used with a developed velocity profile of 1m/s average velocity. At the outlet a pressure boundary condition was used. A no slip wall boundary condition was used for the other two boundaries. Table 2 shows the results of the film thickness as for the middle air bubble considering three initial film thickness: 40, 60 and 80 μm (cases I, II and III) showing some effect on the final value at the middle of the bubble, but no effect on the thinnest value.

Correlation/Simulation	$\delta_{in}[\mu\text{m}]^1$	$\delta_0[\mu\text{m}]^2$	$\delta_{min}[\mu\text{m}]^3$
Moriyama and Inoue	-	69	-
Park and Homsy	-	105	-
Aussilous and Quere	-	70	-
Han and Shikazono	-	64	-
Case I, CLSVOF	89	135	65
Case II, CLSVOF	60	125	65
Case III, CLSVOF	40	115	65

Table 2: A comparison between film thickness predicted by correlations and film thickness obtained by simulations for air bubbles flowing in ethanol.

In the first case, Moriyama and Inoue [26] measured the thickness of the liquid film formed by a growing flattened bubble in a narrow gap whose width ranged from 0.1 to 0.4 mm. They proposed the following correlation to predict the film thickness:

$$\frac{\delta}{d} = \begin{cases} 0.10(\delta^*)^{0.84}, & (Bo > 2) \\ 0.07Ca^{0.41}, & (Bo \leq 2) \end{cases} \quad (3.1)$$

where in Eq. 3.1 δ is the film thickness, d is the tube diameter, Ca is the capillary number ($Ca = \mu U / \sigma$), Bo is the Bond number ($Bo = \rho d^2 U / \sigma$) and δ^* is the ratio between the viscous layer and tube diameter:

¹ The initial film thickness assumed in our simulations

² Film thickness given by correlation, or obtained at the bubble center

³ Minimum film thickness obtained by simulations

A LS method and a HT model implemented into FLUENT for modeling of two phase flows

$$\delta^* = \frac{\sqrt{vt_g}}{d}$$

where t_g is the time required for the bubble edge to reach the measuring point from the bubble initiation. Han and Shikazono [25] proposed the following correlation for the prediction of the liquid film thickness:

$$\frac{\delta_0}{d} = \begin{cases} \frac{0.67Ca^{\frac{2}{3}}}{1 + 313Ca^{\frac{2}{3}} + 0504Ca^{0.672}Re^{0.589} - 0.352We^{0.629}} & (Re < 2000) \\ \frac{106.0\left(\frac{\mu^2}{\rho\sigma d}\right)^{\frac{2}{3}}}{1 + 497.0\left(\frac{\mu^2}{\rho\sigma d}\right)^{\frac{2}{3}} + 7330\left(\frac{\mu^2}{\rho\sigma d}\right)^{0.672} - 5000\left(\frac{\mu^2}{\rho\sigma d}\right)^{0.629}} & (Re > 2000) \end{cases} \quad (3.2)$$

where in Eq. 3.2 Ca is the capillary number, Re is the Reynolds number and We is the Weber number. Park and Homsy [27] developed a theory describing two-phase displacement in the gap between closely spaced planes. They proposed the following correlation for the prediction of the liquid film thickness:

$$\frac{\delta}{d} = 0.669Ca^{2/3} \quad (3.3)$$

Aussilous and Quéré [28] performed a series of experiments at high speeds with liquids of low viscosity in order to determine the liquid film thickness. They proposed the following correlation for the prediction of the liquid film thickness:

$$\frac{\delta_0}{d} = \frac{0.67Ca^{\frac{2}{3}}}{1 + 2.5 \cdot 1.34Ca^{\frac{2}{3}}} \quad (3.4)$$

Table 2 shows the prediction of the liquid film thickness using the above correlations. As can be seen, the experimentally based correlations propose thicknesses ranging from 64 – 105 μm , which fall between the minimum and middle values from the numerical simulation. It is not clear experimentally which values were measured and predicted by their methods. Furthermore, it is expected that a 3D simulation will improve the results (the assumption that the bubble cannot move in the perpendicular plane is eliminated), but nowadays for this case and the mesh used, a 3D simulation is quasi-impossible; the 2D simulation took about 60 days to finish on a 4 processor computer node. Figure 5 depicts the bubble contours in a steady-state condition and Fig 6 presents the initial shape of the bubbles considered in our simulations. Figure 7 shows the presence of a small re-circulating zone near the rear of the middle air bubble. Figure 8 depicts the film thickness (top and bottom) along the middle air bubble. From Fig. 8 we can say that the buoyancy effect is minimal.

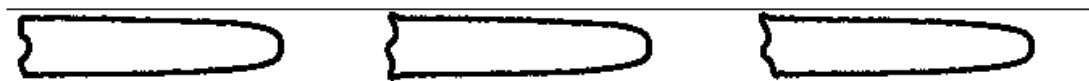


Figure 5: Bubbles contour for the air bubbles flowing inside 1mm tube filled with ethanol.

A LS method and a HT model implemented into FLUENT for modeling of two phase flows



Figure 6: Initial bubbles contour.

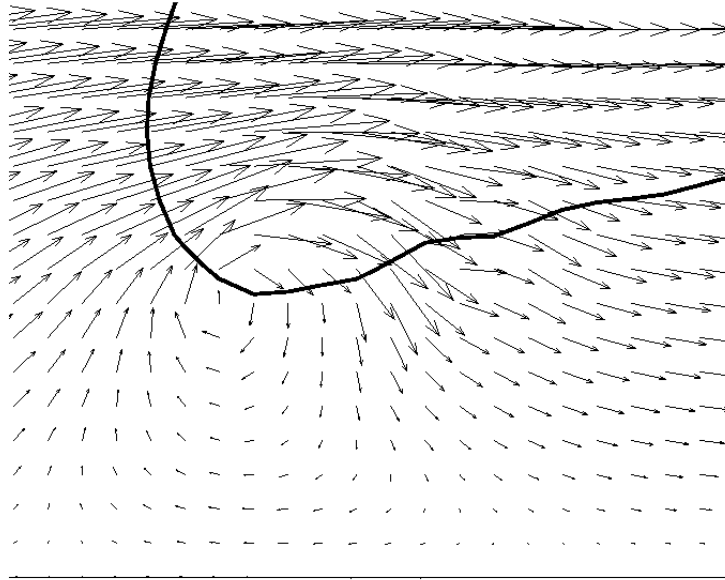


Figure 7: Velocity field near the rear of the middle air bubble.

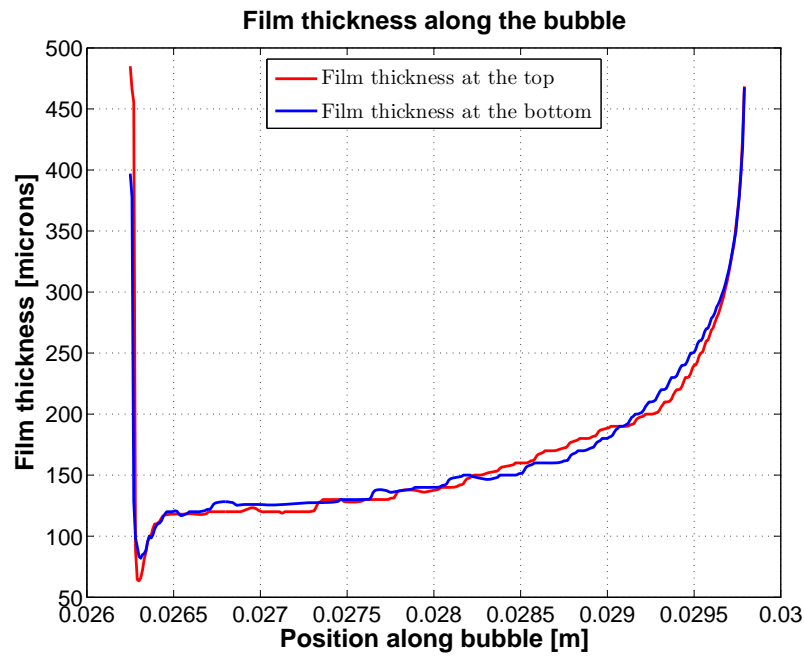


Figure 8: Film thickness along the middle air bubble.

A LS method and a HT model implemented into FLUENT for modeling of two phase flows

3.2 Heat transfer with phase change simulations

In this section, simulations of boiling inside microchannels and small geometries will be presented using water and R134a as working fluids. A 3D computational domain of $800 \times 200 \times 200 \mu m$ was used with a grid of $320 \times 80 \times 80$ and $160 \times 40 \times 40$. The physical properties are given in Table 3.

Fluid	ρ_l <i>kg / m³</i>	ρ_v <i>kg / m³</i>	μ_l <i>μPas</i>	μ_v <i>μPas</i>	c_l <i>J / kgK</i>	c_v <i>J / kgK</i>	k_l <i>W / mK</i>	k_v <i>W / mK</i>	σ <i>N / m</i>
R134a	1187	37.54	185.4	12.04	1446	1065	0.079	0.0173	0.0074
Water	958.4	0.5976	281.8	12.27	4216	2080	0.679	0.0251	0.0589

Table 3: Physical properties of water and R134a.

A small spherical bubble of $20 \mu m$ radius was placed at (0.0002, 0.00002, 0.0001). Water at $102^\circ C$ enters the domain at the left side (see Figure 9) with a uniform velocity of 0.146 m/s . The initial temperature of the vapor phase is $100^\circ C$. All the physical properties are taken at $100^\circ C$. A wall superheat by $8K$ is applied to the bottom wall and a static contact angle of 54° was assumed. A pressure outlet boundary condition was used at the right side of the domain and the other three walls were considered adiabatic.

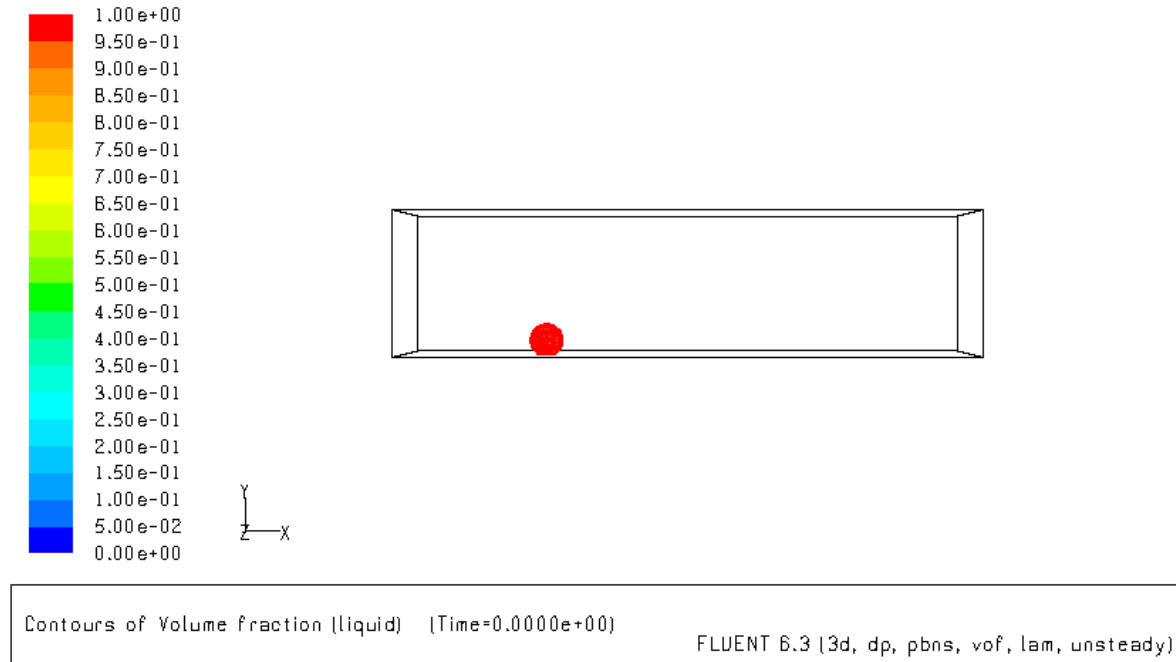


Figure 9: Initial condition for boiling inside microchannels.

Figure 10 shows the bubble contour at different time steps as it grows in the superheated liquid while attached to the superheated wall. Although gravity is present, due to the contact angle and surface tension force, the bubble remains on the heated wall as it grows and eventually occupies the entire cross section of the channel (see Figure 11) and creates dry patches on the lateral walls.

A LS method and a HT model implemented into FLUENT for modeling of two phase flows

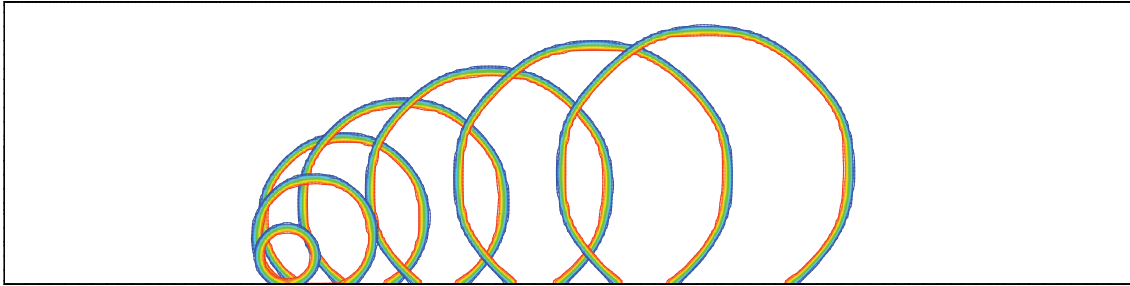


Figure 10: Bubble contour for boiling of water in microchannels, grid 320x80x80.

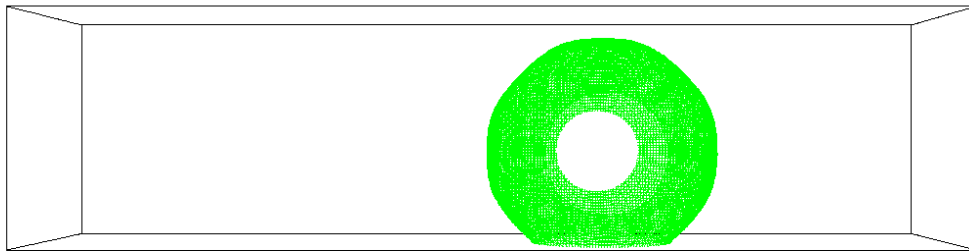


Figure 11: 3D bubble contour with dry patches at the lateral walls, grid 320x80x80.

The same computational domain was used for refrigerant R134a. The liquid enters the domain at $32^{\circ}C$ at the left side with a uniform velocity of 0.05 m/s . The initial vapor phase temperature is $30^{\circ}C$. All the physical properties are taken at this temperature. A wall superheat of 8K is applied to the bottom wall and a static contact angle of 8° was used. A pressure outlet boundary condition was used at the right side of the domain and the other three walls were considered adiabatic. Figure 12 shows the bubble contour at different time steps. Due to the low contact angle, the bubble detaches from the heated wall and therefore the heat and mass transfer process is lower than in the case with water, resulting in a smaller bubble size at the end of the simulation.

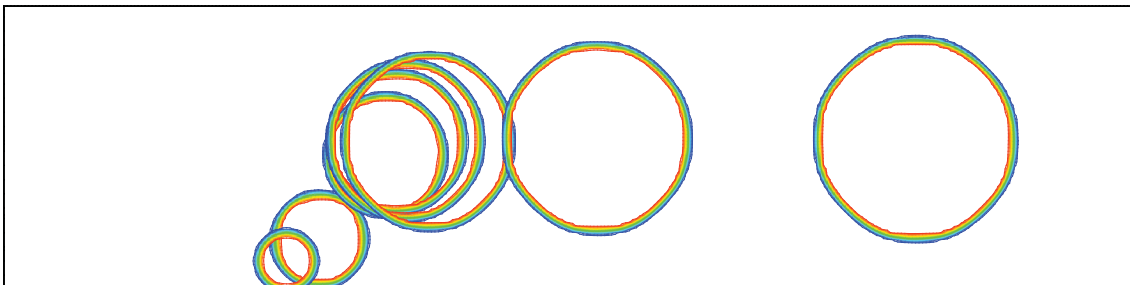


Figure 12: Bubble contour for boiling of R134a in microchannels, grid 320x80x80.

A LS method and a HT model implemented into FLUENT for modeling of two phase flows

A bubble rising from a heated wall was used as another example. A 2D axial symmetric domain of $5 \times 1.25 \text{ mm}$ was used with a grid of 288×72 and 144×36 . A small circular bubble of water at 100° C of $25 \mu\text{m}$ radius was placed in the domain at $(0.0, 0.0)$. The bottom wall was superheated 10K above the saturation temperature, and the surrounding liquid was set initially to 102° C . Since the contact angle is an important parameter in these types of simulations, three contact angles were used: 40° , 54° (the real value) and

80° . Figure 13 depicts the bubble contour at two different time steps when using a contact angle of 40° where due to the low contact angle, the bubble detaches and the growth rate decreases because the bubble is not anymore in contact with the superheated wall. Figure 14 shows the bubble contour when using the real (measured) contact angle of 54° . In this case the bubble remains in contact with the heated wall, and thus the heat and mass transfer are high and the bubble reaches the largest size out of the three simulations. Figure 15 depicts the bubble contour for the contact angle of 80° . The highest heat and mass transfer occurs near the triple line point. In this case the interface between liquid and vapor is almost perpendicular on the heated wall and so the heat and mass transfer are lower than the case of 54° , yielding a smaller bubble than the previous case.

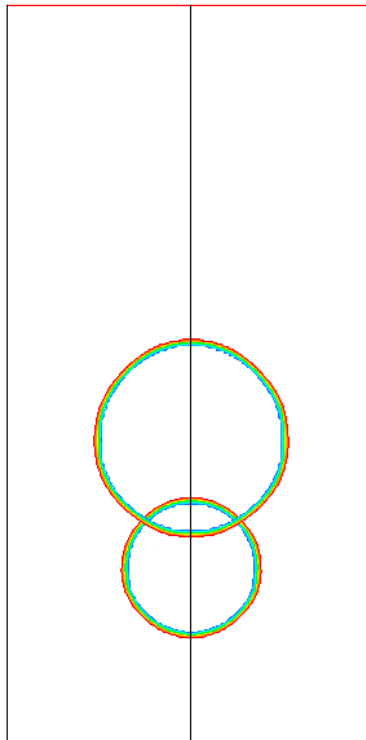


Figure 13: Bubble contour at $t = 0.0625\text{s}$ and $t = 0.125\text{s}$ with a contact angle of 40° , grid 288×72 .

A LS method and a HT model implemented into FLUENT for modeling of two phase flows

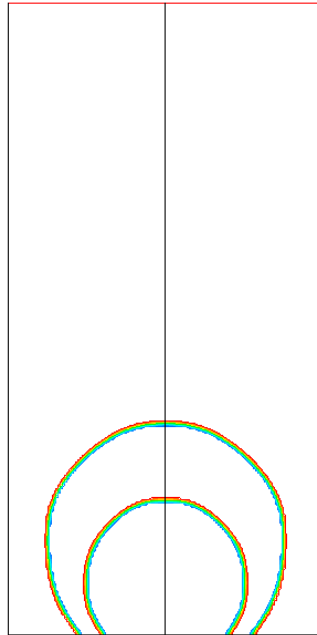


Figure 14: Bubble contour at $t = 0.0625s$ and $t = 0.125s$ with a contact angle of 54° , grid 288×72 .

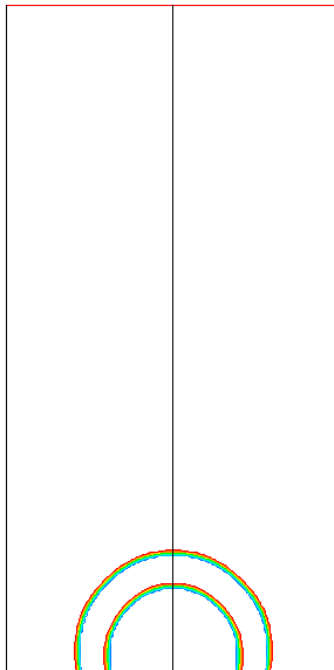


Figure 15: Bubble contour at $t = 0.0625s$ and $t = 0.125s$ with a contact angle of 80° , grid 288×72 .

A LS method and a HT model implemented into FLUENT for modeling of two phase flows

4. CONCLUSIONS

A fully 3D level set method was developed and coupled with the volume of fluid method within the commercial CFD code FLUENT. In this CLSVOF method, the level set function was used to compute the surface tension contribution to the Navier-Stokes equation more accurately than the VOF method by itself. The volume of fluid function was then used to capture the interface. By doing this, we overcame two drawbacks of LS and VOF methods: the mass conservation problem of the LS method, and the rather poor calculation of curvature and normal vector to the interface for the VOF method. A re-initialization equation was solved after each time step for the level set function. This equation was discretized using a fifth order WENO scheme for spatial derivatives and a first order Euler explicit method for time integration. The method was implemented on both serial and parallel solvers.

A film thickness simulation was performed and compared with available correlations in the literature. A qualitative agreement was found.

A heat and mass transfer model was also implemented into the commercial CFD code FLUENT for simulating of boiling (and condensation) heat transfer. Several 3D and 2D axis symmetric simulations were presented with water and R134a as working fluids. The influence of the contact angle was also studied.

5. REFERENCES

- [1] J.U. Brackbill, D.B. Kothe, and C. Zemach. A Continuum Method for Modeling Surface Tension. *Journal of Computational Physics*, 100:335–354, 1992.
- [2] Bogdan A. Nichita. Thesis no 4776 (2010) An improved CFD tool to simulate adiabatic and diabatic two-phase flows, PhD thesis, ÉCOLE POLYTECHNIQUE FÉDÉRALE DE LAUSANNE, <http://library.epfl.ch/theses/?nr=4776>.
- [3] F. Harlow and J. Welch. Volume tracking methods for interfacial flow calculations. *Physics of Fluids*, 8:21–82, 1965.
- [4] J. Donea. Arbitrary Lagrangian-Eulerian finite element methods. *Computational Methods for Transient Analysis*, 1:473–516, 1983.
- [5] C.W. Hirt, A.A. Amsden, and J.L. Cook. An arbitrary Lagrangian-Eulerian computing method for all flow speeds. *Journal of Computational Physics*, 135:203–216, 1997.
- [6] T. Hughes, W. Liu, and T. Zimmermann. Lagrangian Eulerian finite element formulation for incompressible viscous flow. *Computer Methods in Applied Mechanics and Engineering*, 29:239–349, 1981.
- [7] G. Tryggvason, B. Bunner, A. Esmaeeli, D. Juric, N. Al-Rawahi, W. Tauber, J. Han, S. Nas, and Y.-J. Jan. A Front Tracking Method for the Computations of Multiphase Flow. *Journal of Computational Physics*, 169:708–759, 2001.
- [8] Salih Ozen Unverdi and Gretar Tryggvason. A front tracking method for viscous, incompressible, multi – fluid flows. *Journal of Computational Physics*, 100:25–37, 1992.
- [9] C.W. Hirt and B.D. Nichols. Volume of fluid (VOF) method for the dynamics of free boundaries. *Journal of Computational Physics*, 39:201–225, 1981.
- [10] D.L. Youngs. Time dependent multimaterial flow with large fluid distortion. In K. Morton and M. Baines, editors, *Numerical Methods for Fluid Dynamics*, pages 273–285. Academic Press, New York, 1982.
- [11] Jie Li. Piecewise linear interface calculation. *Comptes Rendus de l'Academie des Sciences Serie II. Fascicule B - Mecanique*, 320:391–396, 1995.
- [12] Ruben Scardovelli and Stephane Zaleski. Direct numerical simulation of free surface and interfacial flow. *Annual Review of Fluid Mechanics*, 31:657–603, 1999.
- [13] Mark Sussman, Peter Smereka, and Stanley Osher. A level set approach for computing solutions to incompressible two-phase flow. *Journal of Computational Physics*, 114:146–159, 1994.

A LS method and a HT model implemented into FLUENT for modeling of two phase flows

- [14] Mark Sussman, Emad Fatemi, Peter Smereka, and Stanley Osher. An improved level set method for incompressible two-phase flows. *Computers & Fluids*, 27(5–6):663–680, 1998.
- [15] Mark Sussman, Ann S. Almgren, John B. Bell, Phillip Colella, Louis H. Howell, and Michael L. Welcome. An adaptive level set approach for incompressible two phase flows. *Journal of Computational Physics*, 148:81–124, 1999.
- [16] Mark Sussman and Emad Fatemi. An efficient interface-preserving level set redistancing algorithm and its application to interfacial incompressible fluid flow. *SIAM Journal on Scientific Computing*, 20(4):1165–1191, 1999.
- [17] Mark Sussman. A second order coupled level set and volume-of-fluid method for computing growth and collapse of vapor bubbles. *Journal of Computational Physics*, 187:110–136, 2003.
- [18] Sergey V. Shepel, Brian L. Smith, and Samuel Paolucci. Implementation of a level set interface tracking method in the FIDAP and CFX-4 Codes. *Journal of Fluids Engineering*, 127:674–686, 2005.
- [19] Mark Sussman and Elbridge Gerry Puckett. A coupled level set and volume-of-fluid method for computing 3D and axisymmetric incompressible two-phase flows. *Journal of Computational Physics*, 162:301–337, 2000.
- [20] Gihun Son and Nahmkeon Hur. A coupled level set and volume-of-fluid method for buoyancy-driven motion of fluid particles. *Numerical Heat Transfer, Part B*, 42:523–542, 2002.
- [21] Gihun Son. Efficient implementation of a coupled level-set and volume of fluid method for three dimensional incompressible two-phase flow. *Numerical Heat Transfer, Part B*, 43:549–565, 2003.
- [22] Xiaofeng Yang, Ashley J. James, John Lowengrub, Xiaoming Zheng, and Vittorio Cristini. An adaptive coupled level-set/volume-of-fluid interface capturing method for unstructured triangular grids. *Journal of Computational Physics*, 217:364–394, 2006.
- [23] M. Sussman, K.M. Smith, M.Y. Hussaini, M. Ohta, and R. Zhi-Wei. A sharp interface method for incompressible two-phase flows. *Journal of Computational Physics*, 221:469–505, 2006.
- [24] Sergey V. Shepel and Brian L. Smith. New finite-element/finite-volume level set formulation for modelling two-phase incompressible flows. *Journal of Computational Physics*, 218:479–494, 2006.
- [25] Youngbae Han and Naoki Shikazono. Measurement of the liquid film thickness in micro tube slug flow. *International Journal of Heat and Fluid Flow*, 30:842–853, 2009.
- [26] K. Moriyama and A. Inoue. Thickness of a liquid film formed by a growing bubble in a narrow gap between two horizontal plates. *Journal of Heat Transfer*, 118:132–139, 1996.
- [27] C.-W. Park and G.M. Homsy. Two-phase displacement in hele shaw cells: theory. *Journal of Fluid Mechanics*, 139:291–308, 1984.
- [28] Pascale Aussilous and David Quéré. Quick deposition of a fluid on the wall of the tube. *Physics of Fluids*, 12:2367–2371, 2000.